

## SOME PECULIARITIES OF THE EASTWARD ELECTROJET DISTRIBUTION IN THE EXTREME MAGNETIC STORM ON 10-11 MAY 2024

L.I. Gromova<sup>1</sup>, N.G. Kleimenova<sup>2</sup>, S.V. Gromov<sup>1</sup>, L.M. Malysheva<sup>2</sup>

<sup>1</sup>Pushkov Institute of Terrestrial Magnetism, Ionosphere, and Radio Wave Propagation, Moscow, Troitsk, Russia; e-mail: gromova@izmiran.ru

<sup>2</sup>Schmidt Institute Physics of the Earth RAS, Moscow, Russia

**Abstract.** The magnetic storm on 10-12 May 2024 ( $Dst_{min} = -403$  nT) was the strongest storm in the current 25<sup>th</sup> solar cycle to date. The magnetic storm developed under strong and rapid changes in the structure of the interplanetary magnetic field (IMF). The IMF components changed from negative to positive values (IMF  $B_y$  from  $-40$  up to  $+70$  nT, IMF  $B_z$  from  $-40$  up to  $+50$  nT) under the high speed  $V$  ( $\sim 750$  km/s), and dynamic pressure  $P_{sw}$  ( $\sim 30-35$  nPa) of the solar wind. Here we studied some effects of these IMF changes on the planetary configuration of the ionospheric electrojets and field-aligned currents based on the global maps derived from the magnetic measurements on 66 low orbital satellites of the AMPERE project. An unpredicted large eastward current expansion was found under the strong positive IMF  $B_y$  ( $> +20$  nT) values associated with the appearance of the local very intense upward field-aligned current in the afternoon sector. Some details of new electrojet configurations are discussed.

### 1. Introduction

The magnetic storm on 10-12 May 2024 ( $Dst_{min} = -403$  nT) was the strongest storm in the current 25<sup>th</sup> solar cycle which developed due to a series of large solar flares and coronal mass ejections. By now, many works described solar sources, the solar wind (SW) and interplanetary magnetic field (IMF) parameters, and different aspects of geomagnetic response to this extreme storm have already been published [e.g., Hajra *et al.*, 2024; Kleimenova *et al.*, 2025; Ngwira, 2025; Chernogor, 2025 and references therein].

Throughout the storm, the solar wind and IMF parameters varied significantly in all storm phases. The IMF  $B_y$  changed from  $-40$  up to  $+70$  nT, IMF  $B_z$  changed from  $-40$  up to  $+50$  nT) under the high speed  $V$  ( $\sim 750-900$  km/s), and high dynamic pressure  $P_{sw}$  ( $\sim 10-50$  nPa) of the solar wind. In Fig. 1, one can see variations of the SW and IMF parameters during the interval under consideration and geomagnetic indices of storm  $SymH$  (as 1-min analog of the  $Dst$  index) and auroral activity  $AU$  and  $AL$ . (<https://omniweb.gsfc.nasa.gov/> and <https://wdc.kugi.kyoto-u.ac.jp>).

It was found several  $AU$ -index peaks up to 1600 nT which show maximum magnitude of the eastward electrojet (EE) under the different IMF and SW conditions.

Notes, that such extreme increasing of the  $AU$ -index are rather rare. We analyzed  $AU$  index data from 2000-2025 presented by Wold Data Center in Kyoto and detected that there were only 37 events when the value of the  $AU$  index was around 1000 nT or exceeded this value, and only in 6 events the maximum of the  $AU > 1500$  nT.

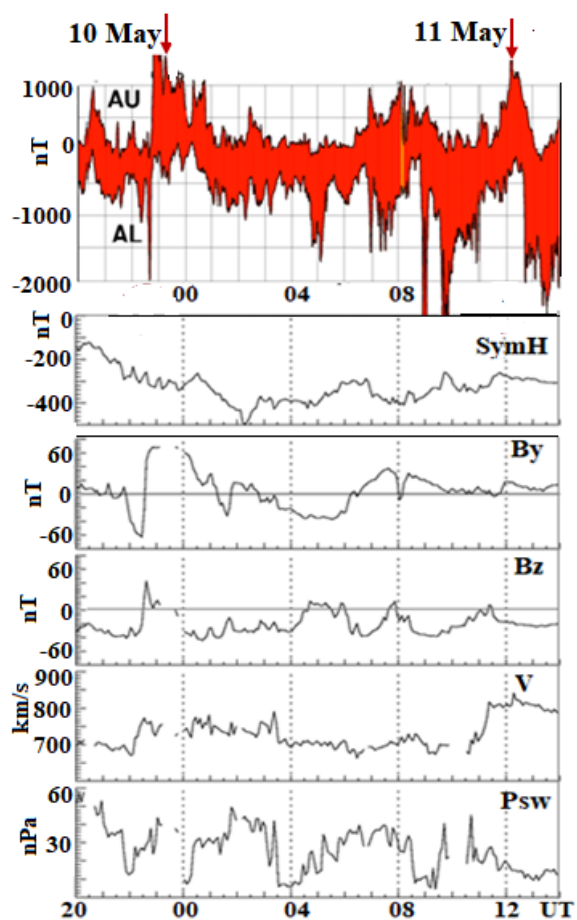


**Figure 1.** Geomagnetic activity indices and the IMF and SW parameters during the interval of the storm 10-11 May under consideration.

Here we studied some effects of strong and rapid IMF and SW changes on the planetary configuration of the eastward electrojet (EE) and accompanying field-aligned currents (FACs) in the daytime-evening sector (09-18 MLT) of the high latitudes. Two events that we analyze in detail are shown in Fig. 1 by the red arrows.

For our study, we used the global maps of the ionospheric currents and field aligned currents basing on the magnetic measurements on the 66 Iridium satellites simultaneously operating at the altitudes of 780 km of the project AMPERE. The maps are presented in the geomagnetic coordinates with a spatial resolution of  $1^\circ$  in MLAT and 1 h MLT in the longitude at 2 min cadence over a ten-minute window (<http://ampere.jhuapl.edu/products>). The magnetic perturbations are given relative to the Earth's main magnetic field with automated baseline, these data are transmitted to the Earth for a spherical harmonic analysis [e.g., Anderson et al., 2000].

## 2. Observations and Discussion

It was found two unpredicted large eastward current expansion. The first one, 22:50 UT on 10 May, shown by the  $AU$ -index peaks up to 1600 nT occurred after rapid simultaneous changing of the IMF  $B_y$  and  $B_z$  from negative values to positive ones. The second  $AU$ -peak up to 1200 nT was observed at 12:10 UT 11 May. It occurred under stable negative  $B_z$  but after rapid change of  $B_y$  from negative values to positive ones.

In the work [Yemori et al., 1979] it is suggested that the ring current and the westward electrojet (WE) are caused by a common mechanism. But the process of development of the eastward electrojet is different from that of WE, or it has a complex process of two or more mechanisms; for example, the effect of the DP-2 current system (which is coherent with variations in the  $B_z$ -component of the IMF) or the effect of the partial ring current values associated with the appearance of the local very intense upward field-aligned current in the afternoon sector.

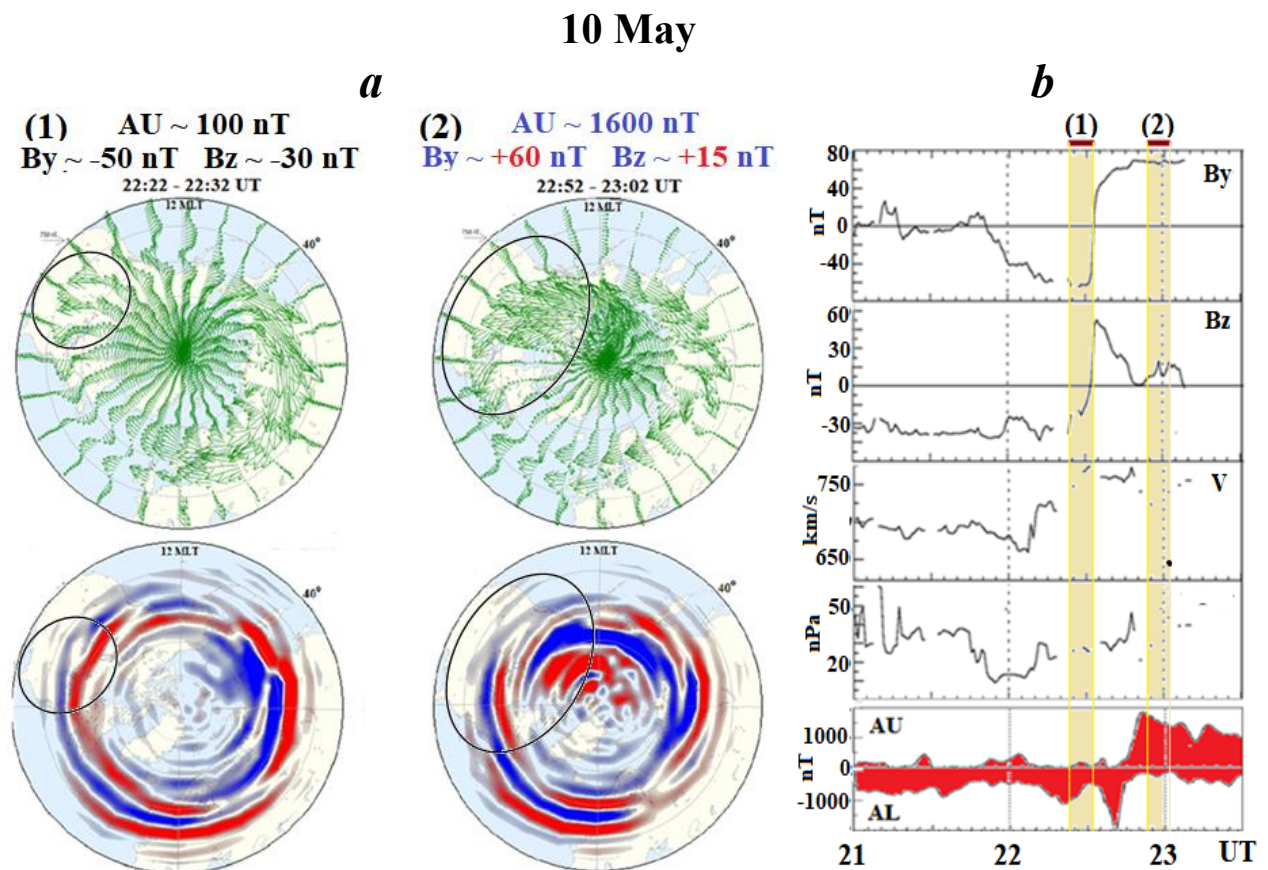


**Figure 2.** The  $AU$ -maximum at 22:50 UT on 10 May: (a) the AMPERE-maps of the ionospheric currents (green vectors) and FACs (upward – red, downward – blue) before (1) and after (2) rapid strong changes the IMF  $B_y$  and  $B_z$ . Black circles show the intensification of the EE and upward FACs; (b) the IMF  $B_y$  and  $B_z$ ,  $V$  and  $P_{sw}$  of the solar wind, indices  $AU$  and  $AL$ . The yellow bars mark the ten-minute data averaging windows corresponding to the maps on the panel (a).

### 2.1 Ionospheric currents before and after the IMF change

In Fig. 2a one can see AMPERE-maps of the ionospheric currents before (left) and after (right) the IMF  $B_y$  and  $B_z$  rapid changing from  $-50$  to  $+70$  nT and  $-40$  to  $+50$  nT correspondingly (so called “flip” according to [Ohtani et al., 2025]) that is shown in Fig. 2b. The eastward electrojet before flip, demonstrated on the left map, significantly intensified, merged with eastward polar current, and expanded from  $55$  to  $\sim 78^\circ$  MLAT in the 13-17 MLT sector (right map). It could be caused by development of partial ring current (PRC). It could be seen significantly weakening of WE previously existing in the post-midnight and morning sectors at latitudes  $50$ - $75^\circ$  MLAT.

At the same time, these strong and rapid changes in IMF led to the significant enhancement and replacement of FACs in the daytime sector of the high latitudes.

### 2.2 Ionospheric currents after the rapid change of the IMF $B_y$ under the IMF $B_z < 0$

As one can see in Fig. 3a (left), the strong eastward electrojet was observed in the daytime sector. After the change of the IMF, the EE location expanded from  $55$  to  $\sim 72^\circ$  MLAT in the 14-19 MLT sector due to the addition of daytime polar currents caused by the appearance of the IMF  $B_y > 0$  (right). The configuration of the field-aligned currents, which enhanced in the afternoon sector of high latitudes, also sharply changed sharply the configuration of the field-aligned currents, which intensified and changed in the afternoon sector of high latitudes.

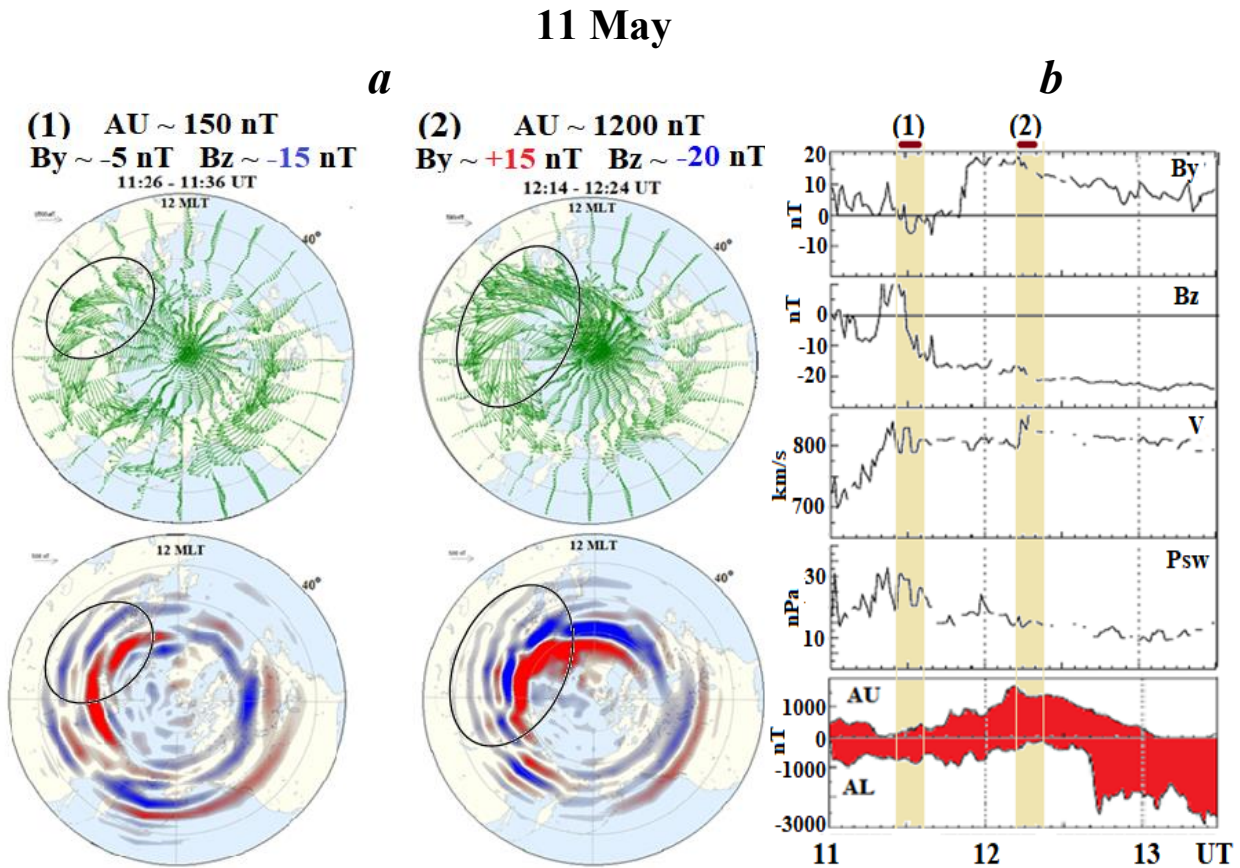


**Figure 3.** The same as in Fig. 2 but for the AU maximum at 12:10 UT on 11 May.

During the considered interval, the IMF  $B_z$  remained negative ( $\sim -20$  nT) that it is shown in Fig. 3b. We assume that the EE enhancement could be caused by an effect of the magnetospheric convection (DP-2 current system) enhanced under  $B_z < 0$ .

The anomalous enhancement of the eastward electrojet observed in both events could be a result of the changes in the azimuthal configuration and size of the afternoon convection cell caused by the emergence of positive IMF values, or an increase of the partial ring current intensity. Previously, in [Gromova et al., 2018], based on the CHAMP satellite data, a fairly high correlation ( $r \sim 0.7$ ) was found between the EE intensity and  $AsymH$  index, which is used as an indicator of the intensity of the partial ring current [Kalegaev et al., 2008], see Fig. 4. However, in the magnetic storm on 10-11 May 2024, no clear coincidence of increases of the AU-index with the variations of the  $AsymH$  indices was found.

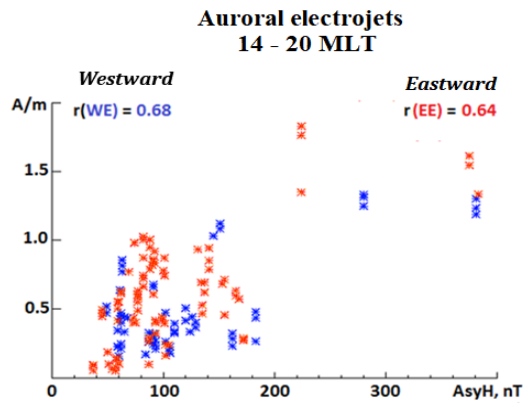


**Figure 4.** Statistical dependence of the intensity of the eastward (red stars) and westward electrojets (blue stars) on *AsyH*-index. Adopted from [Gromova et al., 2018].

### 3. Conclusion

The sharp changes in the IMF structure observed in the magnetic storm 10-12 May 2024 led to significant changes in the structure of the eastward electrojet and field-aligned currents in the daytime-evening sector (09-18 MLT) of high latitudes.

Basing on the global maps of the ionospheric and field-aligned currents derived from the magnetic measurements on 66 low orbital satellites of the AMPERE project it was found:

- the intense eastward electrojet occurred under the strong positive IMF  $B_y$  ( $> +20$  nT), both under the IMF  $B_z > 0$  and IMF  $B_z < 0$ ;
- with an increasing of the positive IMF  $B_y$  value, the eastward electrojet strengthened and latitude ( $55-78^\circ$  MLAT) expanded collocating with the appearance of the local very intense upward field-aligned current.

### References

- Anderson, B.J., Takahashi, K., Toth, B.A. Sensing global Birkeland currents with Iridium® engineering magnetometer data // *Geophys. Res. Lett.* V. 27. P. 4045–4048. 2000. <https://doi.org/10.1029/2000GL000094>
- Chernogor, L.F., Rozumenko, V.T., Shevelev, M.B., Wang, J., Zhang, Y. Global geomagnetic response to the extreme geospace storm of May 10–11, 2024 // *Adv. Space Res.* V. 76. No. 2. P. 939–967. 2025. <https://doi.org/10.1016/j.asr.2025.05.004>
- Gromova, L.I., Förster, M., Feldstein, Y.I., Ritter, P. Characteristics of the electrojet during intense magnetic disturbances // *Ann. Geophys.* V. 36. P. 1361–1391. 2018. <https://doi.org/10.5194/angeo-36-1361-2018>
- Hajra, R., Tsurutani, B.T., Lakhina, G.S., et al. Interplanetary Causes and Impacts of the 2024 May Superstorm on the Geosphere: An Overview // *The Astrophys. J.* V. 974:264. 2024. <https://doi.org/10.3847/1538-4357/ad7462>
- Iyemori, T., Maeda, H., Kamei, T. Impulse Response of Geomagnetic Indices to Interplanetary Magnetic Field // *J. Geomagn. Geoelectr.* V. 31. Iss. 1. P. 1–9. 1979.
- Kalegaev, V.V., Bakhmina, K.V., Alexeev, I.I., Belenkaya, E.S., Feldstein, Y.I., Ganushkina, N.Y. Asymmetry of the ring current during geomagnetic disturbances // *Geomagn. Aeron.* V. 48. P. 780–792. 2008.
- Kleimenova, N.G., Gromova, L.I., Gromov, S.V., Malysheva, L.M. Ground-based geomagnetic disturbances and Pi2 pulsations in the main phase of the superstorm on May 10, 2024 // *Adv. Space Res.* V. 76. No. 12. P. 7533–7545. 2025. <https://doi.org/10.1016/j.asr.2025.04.025>
- Ngwira, C.M., Nishimura, Y., Weygand, J.M., Landwer, L.J., Bush, D.C., Foster, J.C., Erickson, P.J. Evaluating the geomagnetic response to the May 2024 super storm – observations and interpretations // *Front. Astron. Space Sci.* 12:1652705. 2025. <https://doi.org/10.3389/fspas.2025.1652705>
- Ohtani, S., Zou, Y., Merkin, V.G., Wiltberger, M., Pham, K.H., Raptis, S., et al. Ground magnetic response to an extraordinary IMF  $B_y$  flip during the May 2024 storm: travel time from the magnetosheath to dayside high latitudes // *J. Geophys. Res.* V. 130. e2024JA033691. 2025. <https://doi.org/10.1029/2024JA033691>